Multi-Objective Optimization Design of a Notch Filter Based on Improved NSGA-II for Conducted Emissions

LU ZHANG[ID]**1, HONGJUAN GE**[ID]**1, YING MA**[ID]**1, JIANLIANG XUE**[ID]**1, HUANG LI**[ID]**1, AND MICHAEL PECHT**[ID]**2**
[1]College of Civil Aviation, Nanjing University of Aeronautics and Astronautics, Nanjing 210016, China
[2]Center for Advanced Life Cycle Engineering, University of Maryland, College Park, CO 20742, USA

Corresponding author: Hongjuan Ge (allenge@nuaa.edu.cn)

ABSTRACT This paper develops an improved non dominated sorting genetic algorithm II (NSGA-II) based on objective importance vector γ, abbreviated as γ-NSGA-II. Different importance levels for the multiple objectives are incorporated in the objective importance vector, which is applied to determine the individual selection of sorting individuals in the critical layer. And such an individual selection strategy is developed to the NSGA-II algorithm in order to obtain the optimized solution for a task which has multiple objectives with different importance. The differences between the γ-NSGA-II algorithm and the traditional NSGA-II algorithm are discussed in detail. A notch filter is designed for the conducted emission suppression of a transformer rectifier unit (TRU) used in C919 flight testing, and then the parameters optimization design of a notch filter is discussed and conducted based on the γ-NSGA-II algorithm. The non-linear relationship between the filter's parameters and the suppression effect of the conducted emission is also discussed with the help of an electromagnetic compatibility (EMC) evaluation model based on a back propagation (BP) neural network. The experimental results show that the optimized design of the notch filter is effective and the improved γ-NSGA-II algorithm be more specific.

INDEX TERMS Suppression conducted emission, multi-objective optimization, NSGA-II, BP neural network, notch filter, autotransformer rectifier.

I. INTRODUCTION

In recent years, intelligent algorithms have been gradually applied to many new fields, including fault diagnosis, system control, and parameter optimization. [1]–[6]. Liu et al. [1] presented a novel adaptive neural fault-tolerant scheme using finite time convergence, which is the first time the fault-tolerant of switched systems has been considered while maintaining finite-time stability. Liang et al. [2] designed a dynamic containment controller and a static containment controller based on the linear matrix inequality (LMI) method to use in the studied semi-Markovian multiagent systems, respectively. The parameter design for airborne equipment is closely related to the reliability and performance improvement of the equipment. And the application of intelligent algorithms in electrical equipment modeling and parameter optimization has attracted extensive attention [4]–[6].

Non dominated sorting genetic algorithm II (NSGA-II) is a fast non dominated sorting genetic algorithm based on crowded distance, and is a recent research hotspot for multi-objective optimization algorithms. Compared with the non dominated sorting genetic algorithm (NSGA), it not only reduces the computational complexity, but also uses a crowded distance strategy to improve population diversity. The research on improving NSGA-II mainly focuses on computational complexity and population diversity to avoid premature convergence to the local optimum [5]–[15]. NSGA-II was improved by using the local differential method in reference [5], so that its convergence performance is better. Sun et al. [6] combined an improved partheno-genetic algorithm (PGA) with NSGA-II to improve the non dominated sorting and shorten the algorithm's calculation time. Cheng et al. [7] combined the non-revisiting mechanism

based on binary space partitioning with NSGA-II to realize non-repetitive search and save computing resources. In reference [8], the "Neighboring-Max" mode, which not only takes advantage of hybridization but also improves the distribution of the population near the Pareto optimal front, was chosen and used in NSGA-II on the basis of a hybridization-encouraged mechanism. Deb and Himanshu [14], [15] proposed the non dominated sorting genetic algorithm III (NSGA-III) based on reference-point. NSGA-III no longer uses the crowded distance strategy, but analyzes individuals more systematically based on reference-point in the critical layer to select the next generation. NSGA-III solves the problems of poor convergence and individual diversity of NSGA-II in multi-objective optimization tasks with three or more objectives.

However, current improvement research seldom takes the impact of the importance of each objective on population evolution into account. In engineering applications, the importance of objectives is different in a multi-objective optimization task, and the importance of objectives in the same task may also change according to the users. The evolution process of NSGA-II cannot reflect the emphasis on more important objectives when the importance of each optimization objective is different. Liu *et al.* [16] used a weighted scale method to select a compromise solution from the Pareto optimal solution. Although the weight of each optimization objective can be considered, the evolution process of the NSGA-II algorithm itself was not improved, and the weight setting was not objective enough. This paper develops an improved NSGA-II algorithm based on objectives importance vector γ and an an individual selection strategy of dimension reduction sorting for individuals in the critical layer. Then the Pareto optimal solution obtained by the evolution of γ-NSGA-II is compared with the result before improvement, which verifies the superiority of γ-NSGA-II in completing optimization tasks with high-dimensional objectives of different importance.

This paper designs a conducted emission suppression unit of a transformer rectifier unit (TRU) used in the power supply system of C919 flight test equipment. The parameter selection process is used as an example to research the application of the γ-NSGA-II algorithm. In order to solve the problem of conducted interference on the equipment, it is necessary to build an evaluation model for conducted interference and determine an effective suppression scheme for conducted emissions. The research on simulation modeling of electronic components and functional modules of interference sources is more common among the existing evaluation methods of conducted emissions [17]–[23]. With the increasing complexity of actual electromagnetic environments, it is difficult for modeling and simulation based on physical characteristics to evaluate electromagnetic interference (EMI) comprehensively and accurately. Therefore, some research builds mathematical models based on data to predict and evaluate EMI. Wu and Wei [24] took advantage of a back propagation (BP) neural network to simulate the interference current

waveform of electro-static discharge (ESD). Li *et al.* [25] used a BP neural network to obtain the mapping between input predictors and the interference responses of sensitive devices through selecting effective EMI parameters as input predictors. Zhou *et al.* [26] selected an appropriate BP neural network structure to build an electromagnetic interference damage model of a low-dropout (LDO) linear voltage regulator and predicted the impact of electromagnetic interference on LDO output voltage. These studies provide solutions to specific problems related to EMI.

Qian and Chen [27] installed a notch filer on the power supply side to filter conducted emission signals of specific frequencies, which can prevent the interference generated by equipment from being transmitted to the power grid side through the power lines, thereby ensuring that the equipment meets the requirements of conducted emission. At present, it is difficult for notch filter parameters determined by suppression frequency and engineering experience to achieve optimal performance taking conducted emission suppression, operational performance, and installation cost into account concurrently. Wang *et al.* [28] applied an S parameter to predict noise attenuation under impedance mismatch conditions, leading to a better high-frequency performance of the filter. Chang and Ko [29] proposed a particle swarm optimization algorithm with nonlinear time-varying evolution based on neural network (PSO-NTVENN), which optimizes the filter cost, filter loss, current, and voltage total harmonic distortion (THD). Lu *et al.* [30] evolved the population to the optimal coordination point of multi-objectives through threshold restriction of the fitness function of the genetic algorithm. However, the current research mainly focuses on the optimization of the filtering effect and reactive power compensation of the filter, and the optimized design aimed at EMI suppression has not been discussed.

As a multi-objective optimization algorithm, γ-NSGA-II introduces an objectives importance vector γ based on the NSGA-II algorithm, then reduces the dimension of the γ according to the importance of each objective and carries out fast non-dominant sorting for individuals in the critical layer. In addition, the optimized design of parameters of the conducted interference notch filter is applied as an example to analyze the application of the improved algorithm. This paper is organized as follows. Section II introduces the objectives importance vector γ into the traditional NSGA-II algorithm. In section III, the conducted emission of the power line of a 12-pulse autotransformer rectifier unit (ATRU) is measured according to the electromagnetic compatibility (EMC) standard GJB152A [31], and the EMI suppression scheme and optimization objectives of the notch filter parameters are defined. In section IV, an evaluation model of conducted interference suppression based on BP neural network is established, and fitness functions corresponding to each objective of this example are created. Section V includes the simulation and experimental research of conducted interference, which verifies the superiority of the proposed γ-NSGA-II algorithm. Section VI presents conclusions.

II. IMPROVEMENT OF NSGA-II ALGORITHM

NSGA is a multi-objective optimization genetic algorithm based on Pareto optimality. To reduce the time complexity and improve the population diversity, NSGA-II was developed.

A. THE DEVELOPMENT OF NSGA-II

NSGA adopts the non-dominant stratification method, so that the better individuals have a greater chance to proceed to the next generation. The fitness sharing strategy enables individuals in the critical layer to distribute evenly, overcomes the over-reproduction of super individuals, and prevents premature convergence. But application of the NSGA algorithm exposes the following shortcomings. a.

1) The time complexity of non dominated sorting is very high, and the worst case is $O(mn^3)$. Among them, m is the number of objective functions and n is the population size.
2) The elite strategy is not supported. This strategy demonstrates good performance in maintaining good individuals and accelerating convergence to the Pareto set.
3) The shared parameters need to be assigned artificially, which will have a significant impact on population diversity.

As an improved algorithm of NSGA, NSGA-II overcomes the above shortcomings. A fast non dominated sorting algorithm is developed to reduce the time complexity of the sorting algorithm to $O(mn^2)$. The congestion distance algorithm and elite strategy are used to replace the shared function algorithm in NSGA, so that the performance of diversity maintenance is no longer dependent on the assigned shared parameters.

However, the NSGA-II algorithm does not take into account the impact of the importance of each target on population evolution. In fact, whether it is the biological evolution of nature or the application of genetic algorithm to solve engineering problems, the importance of optimization objectives should be reflected in the population evolution.

B. IMPROVED NSGA-II WITH TARGET IMPORTANCE VECTOR

The flowchart of γ-NSGA-II is shown as Fig. 1. The elements of the target importance vector γ are the optimization objectives of the arrangement of the importance from high to low. Let four optimization objectives be T_1, T_2, T_3, T_4, then $\gamma = [T_1, T_2, T_3, T_4]$.

As shown in the flowchart, the paternal population P_t whose number of individuals is N is randomly generated, and its individuals are sorted using the fast non dominated sorting approach. By selection, crossover, and mutation of individuals in P_t, a sub-population Q_t with individual number N is formed. The parent population P_t and the offspring population Q_t are merged as population R_t, the size of R_t is $2N$.

We need to select N optimal individuals from R_t to form the new parent population P_{t+1}. R_t is divided into n
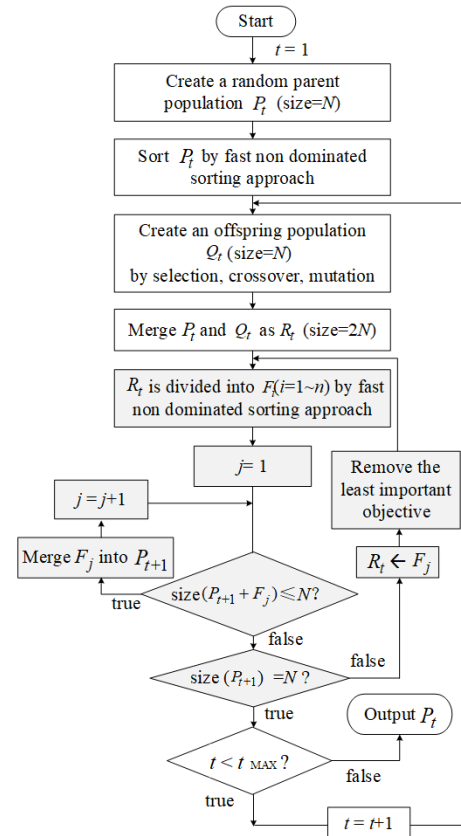

FIGURE 1. Flow diagram of γ-NSGA-II algorithm.

non-dominating layers $(F_1, F_2, \ldots, F_n)$ by a fast non dominated sorting approach. If the total number of individuals in $F_1, F_2, \ldots, F_{l-1}$ is L $(L<N)$, then the total number of individuals in $F_1, F_2, \ldots, F_l$ is more than N. Thus, there are $(N\text{-}L)$ individuals in F_l that should be selected for the new parent population P_{t+1}. All of the optimization objectives are contained in objective vector $\mathbf{M}$ and are sorted in descending order of importance. The least important objectives are removed from $\mathbf{M}$, and the individuals of F_1 are divided into x non-dominating layers $(H_1, H_2, \ldots, H_x)$ by a fast non dominated sorting approach. If the total number of individuals in $H_1, H_2, \ldots, H_{k-1}$ is K $(K<N\text{-}L)$, while the total number of individuals in $H_1, H_2, \ldots, H_k$ is more than $(N\text{-}L)$, the least important optimization objectives from $\mathbf{M}$ are removed and the individuals of H_k by fast are layered by a non dominated sorting approach. These steps are repeated until the total number of individuals in P_{t+1} is equal to N.

The improved algorithm follows the main framework of NSGA-II. To avoid repetition, the same part of the main loop is not described in details, and the selection method of critical layers is mainly introduced, whose pseudocode is as follows.

In this paper, the parameter optimization design of a conductive interference notch filter is used as an example to study the application of γ-NSGA-II. In different application situations, notch filters have different target importance vectors. If the notch filter is used to suppress the conducted

Algorithm 1 Dimension Reduction By Importance(**P**,**M**,**N**)

input
  P: set of population in critical layer,
  M: objective vector (importance in descending order),
  N: the number of Chromosomes need to be selected

Output **Pselected**: set of selected population

1:     **F** $\leftarrow$ FastNondominatedSort(**P**,**M**)
2:     $m \leftarrow 0, i \leftarrow 0$
3:     **while** i $<$ **F**.length() **do**
4:         m $\leftarrow$ **F**[i].length() $+$ m
5:         **if** $m \leq$ N **then**
6:             **F**[i] into **Pselected**
7:             $i \leftarrow i+1$
8:         **else** break
9:         **end if**
10:     **end while**
11:     **if Pselected**.length() $<$ N **then**
12:         **M** $\leftarrow$ remove the last element of **M**
13:         DimensionReductionByImportance(**F**[i], **M**,N-m)
14:     **end if**
15:     **return Pselected**

FIGURE 2. Test results of TRU power line conducted emissions without notch filters.
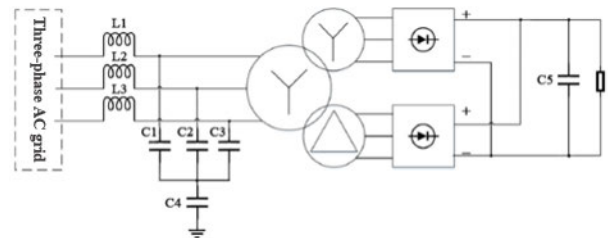
FIGURE 3. 12-pulse TRU for C919 flight test power supply system.

emissions of power supply equipment in flight testing, its volume and weight should be minimized and the importance of its economy should be minimized on the premise of ensuring that EMC meets the standard. However, for notch filters that need batch production and are installed in civil equipment, economy is obviously more important, while the optimization of volume and weight may become insignificant. The γ-NSGA-II algorithm distinguishes the two optimization requirements.

III. MEASUREMENT AND SUPPRESSION OF CONDUCTED EMISSIONS

In order to verify the effectiveness of γ-NSGA-II for optimization of multi-objectives with different importance, the optimal design of conducted emission suppression for the 12-pulse TRU is used as an example.

A. MEASUREMENT OF POWER LINE CONDUCTED EMISSIONS

According to the test item CE102 ''10 kHz-10 MHz power line conducted emission'', the EMC standard GJB152A, the 12-pulse TRU used in the power supply system of C919 flight test equipment was the research object, and EMC testing was carried out. In the frequency range of 10 kHz-10 MHz, the transmission interference of the equipment must be less than the allowable threshold.

The structure of the test equipment is shown in Fig. 3. The rated frequency of the TRU in the power supply system of test flight equipment is 400 Hz, and its working frequency range is 360 Hz-800 Hz. The main reasons for the transmission interference are the THD of the input current of the transformer and the high transient voltage
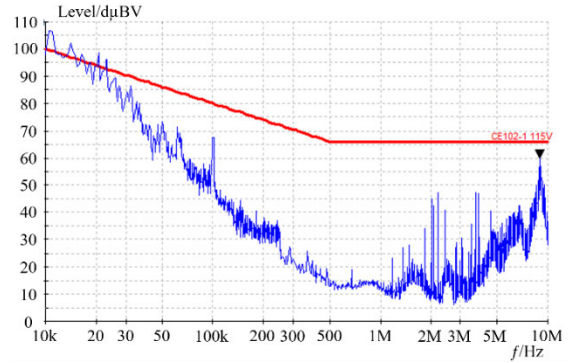
(dv/dt) and high transient current (di/dt) generated by the switching-on of the rectifier bridge diode [32][33]. The blue curve in Fig. 2 is the test result of the conducted emissions of the TRU without notch filters shown in Fig. 3. The input source is 115 V/400 Hz, and the load current is 150 A in the test experiments. In Fig. 2, the red curve indicates the allowed boundary of the conducted emissions, and it is from the standard CE102 requirement of GJB152A. The test results, show that the conducted emissions in the range from 10 kHz to 30 kHz are over the boundary value. In order to suppress the conducted emissions and make them meet the standard requirements, it is necessary to design a notch filter to filter the interference level in this frequency band and transmit the 400 Hz power to the load without attenuation.

B. CONDUCTED EMISSION SUPPRESSION METHOD AND OPTIMIZATION OBJECTIVES

Passive filters have been widely used in passive harmonic control and electromagnetic interference suppression in the aviation field because of their small volume, weight, and high reliability. Among them, the application of single-tuned filter is the most mature. In Fig. 4, a notch filter consisting of n single-tuned filters in parallel can filter the interference signals at n frequency points.

The complex impedance of the ith single-tuned filter in Fig. 4 is:

$$Z_i = R_i + j(\omega L_i - \frac{1}{\omega C_i}) = R_i + j(X_{L_i} + X_{C_i})$$
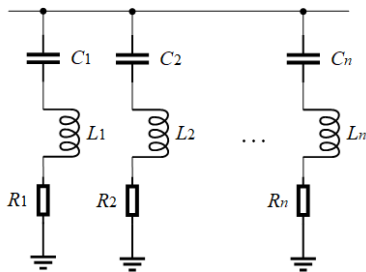$$= R_i + jX_i \tag{1}$$

FIGURE 4. Topology of notch filter.

In which, ω is the angular frequency, R, L, and C are the values of resistance, inductance and capacitance of the single-tuned filter, respectively. Eq. (2) shows that the resonant frequency f_0 of the circuit is only related to the values of L and C. When the frequency of the external excitation signal is consistent with the resonant frequency of the circuit, the current flows into the filter, and seldom flows to the load. To suppress the conducted interference in a specific frequency band, this characteristic can be used to prevent the interference level from flowing into the power grid.

$$f_0 = \frac{1}{2\pi\sqrt{LC}} \tag{2}$$

The resonant curve of the filter shows the relationship between the current and the angular frequency. The resonant curve peaks at the resonant frequency f_0, where the current value of the flow filter is the largest. The selectivity of the resonant circuit depends on the quality factor Q. The larger the Q value, the sharper the curve near the peak value, and the better the selectivity of the circuit.

$$Q = \frac{1}{R}\sqrt{\frac{L}{C}} \tag{3}$$

If the values of f_0 and Q can be determined, only the relationship between R, L, and C can be obtained according to eqs. (2) and (3). Normally, the parameters of a notch filter can be determined according to suppression frequency and engineering experience, which makes it difficult to achieve multi-objective optimal parameter design.

According to the results of the EMC test in Fig. 2, the target frequency band of the study was determined to be 10 kHz - 30 kHz. A notch filter must be able to eliminate the interference in this frequency band. Based on the requirements, four optimization objectives of the notch filter are proposed: conducted emission margin (ΔCE), THD of conducted emission (CE_{THD}), weight of the notch filter, and cost of the notch filter. The definitions of ΔCE and CE_{THD} are as follows.

(1) Conducted emission margin: ΔCE refers to the minimum difference between the limit level and the transmitted signal in the target frequency band. The higher the ΔCE value, the better the suppression effect of the conductive emission. If the transmitted signal exceeds the limit level

curve at a certain frequency point, ΔCE is negative, and the electromagnetic compatibility of the equipment is not up to the standard.

(2) THD of conducted emission: CE_{THD} refers to the square sum of the harmonic components U_i divided by the fundamental components U_1 in the target frequency band as shown in eq. (4).

$$CE_{THD} = \sqrt{\sum_{i=n}^{N}\left(\frac{U_i}{U_1}\right)^2} \tag{4}$$

IV. CONDUCTED EMISSION EVALUATION MODEL BASED ON BP NEURAL NETWORK

Because of the complexity of the electromagnetic environment, ΔCE and CE_{THD} can not be calculated by physical formula. If the simulation model of conducted interference measurement is established, the ΔCE and CE_{THD} corresponding to different notch filter parameters can be obtained by simulation. However, new chromosomes will appear in each generation of genetic algorithm. If the ΔCE and CE_{THD} of each new chromosome are obtained by simulation, it will consume a lot of time and the time complexity of the algorithm is unacceptable. BP neural network has good generalization ability. After limited training, it can be used to predict ΔCE and CE_{THD} under different notch filter parameters.

A. CHROMOSOME CODING

Chromosome coding should contain all the genetic information required. On the one hand, according to eqs. (2) and (3), L and C can be calculated by R, f, and Q. On the other hand, the initial range of f, which is necessary for generating the input data of γ-NSGA-II, can be estimated directly from the results of the EMC test without notch filters (Fig. 2), and the initial range of Q can be determined by engineering experience. Therefore, a chromosome of a notch filter should be composed of R, f, and Q of each single-tuned filter in the notch filter. A notch filter contains k sets of single-tuned filters, so the ith chromosome X_i is a gene chain containing $3k$ genes. As shown in eq. (5), R_{ij}, f_{ij}, and Q_{ij} represent the resistance, resonant frequency, and quality factor of the jth single-tuned filter, respectively. The range of j is $[1, k]$.

$$X_i = [R_{i1}, f_{i1}, Q_{i1}, R_{i2}, f_{i2}, Q_{i2}, \ldots, R_{ik}, f_{ik}, Q_{ik}]^T \tag{5}$$

B. NEURAL NETWORK STRUCTURE AND ACCURACY VERIFICATION

The BP neural network structure with m hidden layers is shown in Fig. 5. Eqs. (6) and (7) give the input and output vectors of the neural network, respectively. The number of elements in the input vector is $3k$, where k is the number of single-tuned filters in a notch filter.

Therefore, the input layer of the neural network has $3k$ neurons, including the resistance value, resonant frequency, and quality factor of k single-tuned filters. The two neurons in the output layer are ΔCE and CE_{THD} corresponding to the
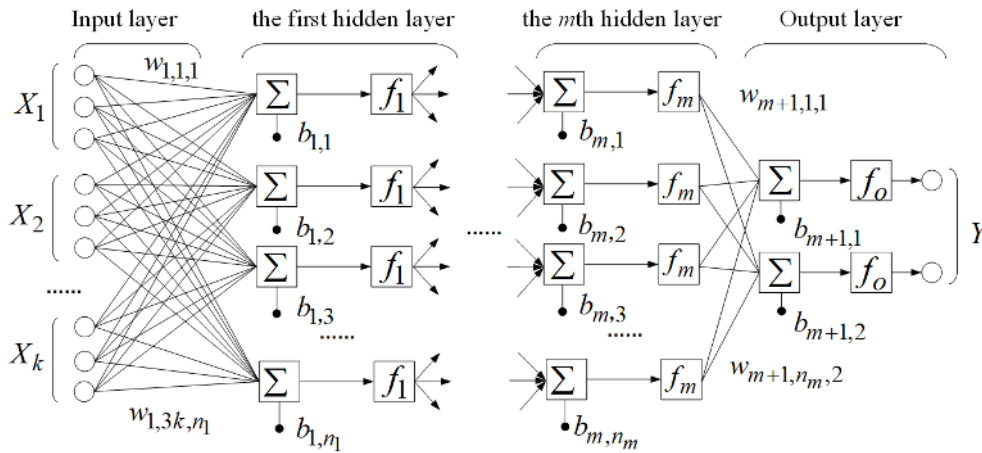
FIGURE 5. Structure of neural network for conducted emission suppression evaluation.

TABLE 1. Mean absolute percentage errors (MAPES) of three sets of simulation experiments.

Number of Single-tuned Filters	MAPE	
	ΔCE	CE_{THD}
1	3.5%	4.6%
2	4.9%	4.9%
3	3.6%	3.9%

input notch parameters. The number of nodes in each hidden layer in Fig. 5 is $n_1, n_2, \ldots, n_m$. The weights and biases are expressed in w and b, respectively.

$$X = [X_1, X_2, \ldots, X_k]$$
$$= [R_1, f_1, Q_1, R_2, f_2, Q_2, \ldots, R_k, f_k, Q_k] \quad (6)$$
$$Y = [\Delta CE, CE_{THD}] \quad (7)$$

Therefore, the mapping relationship between notch filter parameters and ΔCE and CE_{THD} can be obtained by training the BP neural network.

To verify the accuracy of the BP neural network, the simulation model of 12-pulse TRU for conducted emission measurement was established by MATLAB/Simulink. Three sets of simulations were conducted. In the first set of simulations, one single-tuned filter was connected in parallel in each phase of the power line; in the second set, two single-tuned filters were connected in parallel in each phase; and in the third set, three single-tuned filters were connected in parallel in each phase. Eq. (6) is the input data, and eq. (7) is the output data. For each set of simulations experiments, 5000 sets of data were obtained and divided into training sets, verification sets, and test sets. After the trained BP neural networks for each set of simulation were obtained, mean absolute percentage error (MAPE) was used to measure the relative errors on the test sets to verify the accuracy of the BP neural network.

As shown in Table 1, the MAPEs of ΔCE and CE_{THD} are less than 5%, which is acceptable for our optimization design task.

C. FITNESS FUNCTION ANALYSIS

The fitness functions of four optimization objectives of the notch filter parameters (ΔCE, CE_{THD}, W_F, C_F) were established as follows.

The fitness function of ΔCE is eq. (8), where c is a constant that makes $F_{\Delta CE}(X_i)$ positive.

$$F_{\Delta CE}(X_i) = \text{c} - \Delta CE \quad (8)$$

The fitness function of CE_{THD} is eq. (9).

$$F_{CE_{THD}}(X_i) = CE_{THD} \quad (9)$$

W_F is the sum of the weight of resistance, inductance, and capacitance of each single-tuned filter in the notch filter. It is calculated by eq. (10), where k is the parallel number of single-tuned filters, j is the sequence number of single-tuned filters, and w_1, w_2 and w_3 are the unit weight factors of resistance, inductance, and capacitance, respectively.

$$W_F(X_i) = \sum_{j=1}^{k} (w_1 R_{ij} + w_2 L_{ij} + w_3 C_{ij}) \quad (10)$$

C_F is the sum of the cost of resistance, inductance, and capacitance of each single-tuned filter in the notch filter. It is calculated by eq. (11), where k is the parallel number of single-tuned filters, j is the sequence number of single-tuned filters, and α_1, α_2, and α_3 are the unit cost factors of resistance, inductance, and capacitance, respectively[30][34].

$$C_F(X_i) = \sum_{j=1}^{k} (\alpha_1 R_{ij} + \alpha_2 L_{ij} + \alpha_3 C_{ij}) \quad (11)$$

V. SIMULATION AND EXPERIMENTAL VERIFICATION

In order to verify the correctness of the theoretical analysis, simulation experiments are used for comparative study.

A. ALGORITHM RESULTS COMPARISON

According to the EMC test results of the TRU without notch filters in Fig. 2, the target frequency range where EMI needs
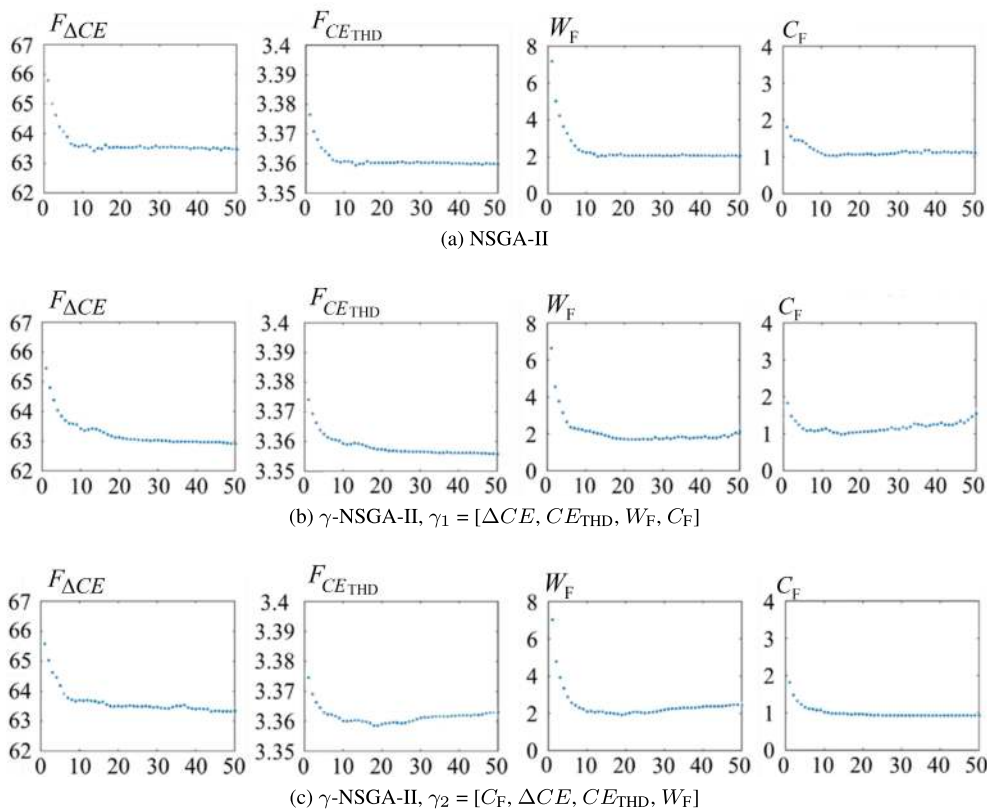
FIGURE 6. Evolutionary process of fitness value before and after algorithm improvement.

to be suppressed is 10 kHz-30 kHz. One single-tuned filter can only suppress EMI in a narrow frequency range, so more than one single-tuned filter should be designed to suppress EMI in the 10 kHz-30 kHz range. The results of the simulations conducted in Section IV show that at least three single-tuned filters connected in parallel are necessary to make ΔCE positive and to achieve satisfactory results.

Combined with the target frequency range (10 kHz-30 kHz) and engineering experience, the initial ranges of notch filter parameters are shown in Table 2. To ensure the effectiveness of conducted emission suppression and make genetic evolution converge faster, R, f, and Q are randomly generated within their respective initial ranges when the population is initialized.

TABLE 2. Initialization value range of notch filter parameters.

Parameter	Minimum	Maximum
f	10 kHz	30 kHz
R	3 Ω	5 Ω
Q	0.5	2

In the ith simulation, three groups of notch filter parameters are generated randomly according to the range given in Table 2, and the parameters vector of the notch filter is formed as eq. (12). The simulation result vector is shown as

eq. (13). $[X, Y]$ constitutes the sample data of the BP neural network.

$$X_i = [R_{i1}, f_{i1}, Q_{i1}, R_{i2}, f_{i2}, Q_{i2}, R_{i3}, f_{i3}, Q_{i3}] \quad (12)$$
$$Y_i = [\Delta CE_i, CE_{\text{THD}i}] \quad (13)$$

In the range given in Table 2, the initial population with 50 individuals is randomly generated. The genetic information of each chromosome is used as the input of the neural network, and the output is the corresponding ΔCE and CE_{THD}. And eqs. (8), (9), (10), and (11) are used to calculate the corresponding fitness values of the four objectives.

After 50 iterations using the traditional NSGA-II algorithm, the average values of four optimization objectives of Pareto solution sets of each generation are shown in Fig. 6(a). For comparative analysis, γ-NSGA-II is utilized for 50 iterations with γ_1 and γ_2 as the optimized objectives vectors, respectively. The averages of four optimization objectives of the Pareto solution sets of each generation are shown in Fig. 6(b) and Fig. 6(c).

$$\gamma_1 = [\Delta CE, CE_{\text{THD}}, W_{\text{F}}, C_{\text{F}}] \quad (14)$$
$$\gamma_2 = [C_{\text{F}}, \Delta CE, CE_{\text{THD}}, W_{\text{F}}] \quad (15)$$

Comparing the evolutionary processes of populations in the three situations shown in Fig. 6 leads to the following three observations.

TABLE 3. Comparison of the 50th generation Pareto solution set before and after algorithm improvement.

	NSGA-II with all of the objectives				γ-NSGA-II $\gamma_1 = [\Delta CE, CE_{THD}, W_F, C_F]$				γ-NSGA-II $\gamma_2 = [C_F, \Delta CE, CE_{THD}, W_F]$				NSGA-II with two objectives	
	$F_{\Delta CE}$	$F_{CE_{THD}}$	W_F	C_F	$F_{\Delta CE}$	$F_{CE_{THD}}$	W_F	C_F	$F_{\Delta CE}$	$F_{CE_{THD}}$	W_F	C_F	$F_{\Delta CE}$	$F_{CE_{THD}}$
1	63.441	3.359	2.010	1.054	62.919	3.356	1.904	1.381	63.364	3.362	2.393	0.947	62.723	3.352
2	63.426	3.360	2.229	1.051	62.867	3.356	1.901	1.425	63.314	3.362	2.346	0.934	62.767	3.351
3	63.428	3.358	2.123	1.067	62.911	3.356	2.010	1.297	63.483	3.363	2.491	0.941	62.823	3.351
4	63.423	3.359	2.039	1.095	62.934	3.356	1.984	1.364	63.426	3.363	2.510	0.939	62.921	3.349
5	63.442	3.359	2.101	1.109	62.931	3.356	1.861	1.278	63.346	3.362	2.337	0.936	62.751	3.352
6	63.555	3.360	2.057	1.098	62.898	3.356	1.818	1.743	63.387	3.363	2.415	0.954	62.781	3.352
7	63.594	3.360	2.118	1.066	62.893	3.356	2.097	1.543	63.306	3.362	2.342	0.942	62.881	3.352
8	63.477	3.360	2.072	1.076	62.923	3.356	2.210	1.689	63.324	3.363	2.484	0.934	62.932	3.351
9	64.389	3.360	2.051	1.057	62.872	3.356	1.885	1.496	63.355	3.363	2.384	0.933	62.812	3.352
10	63.469	3.359	2.030	1.052	62.880	3.356	1.980	1.372	63.311	3.362	2.464	0.931	62.779	3.351
11	63.496	3.360	2.026	1.082	62.910	3.356	2.148	1.539	63.346	3.363	2.338	0.935	62.831	3.350
12	63.470	3.359	2.045	1.085	62.893	3.356	2.244	1.599	63.351	3.362	2.382	0.929	62.712	3.352
Avg	63.468	3.359	2.070	1.074	62.903	3.356	2.004	1.478	63.359	3.363	2.407	0.937	62.809	3.351

* Note: Under the condition of NSGA-II with two important objectives, the average values of W_F and C_F are 3.101 and 2.712, respectively.
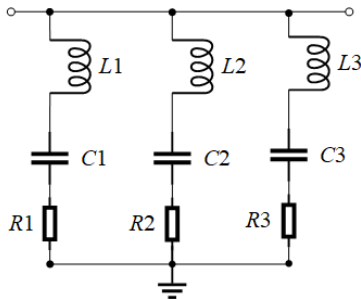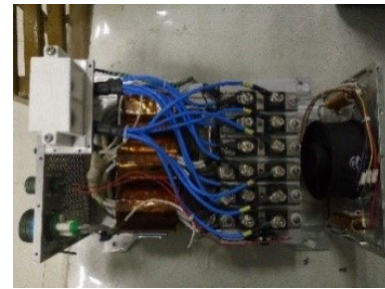

FIGURE 7. Notch filter for only the A phase of the 12-pulse TRU.

(a) Prototype of 12-pulse TRU

(b) Notch filters for the A, B, and C phases of 12-pulse TRU
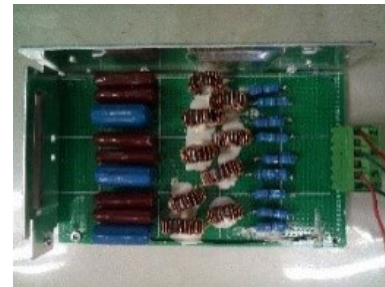
FIGURE 8. Physical diagrams of TRU and notch filters.

(1) From Fig. 6(b), which shows the evolutionary process of the γ-NSGA-II algorithm, it can be seen that in the condition of $\gamma_1 = [\Delta CE, CE_{THD}, W_F, C_F]$, the two less important optimized objectives, W_F and C_F, show a slight upward trend in the later evolution stage, which makes the values of $F_{\Delta CE}$ and $F_{CE_{THD}}$ lower, and meets the needs of users who have strict requirements for EMI suppression and low requirements for economic costs.

(2) From Fig. 6(c), it can be seen that in the condition of $\gamma_2 = [C_F, \Delta CE, CE_{THD}, W_F]$, the least important optimized objective, W_F, shows a slight upward trend in the later evolution stage, while reducing the C_F value to a lower level to meet the needs of users who regard the lowest economic cost as the most important optimal objective.

(3) However, as shown in Fig. 6(a), each objective shows a downward trend in the evolutionary processes of the NSGA-II algorithm. Comparing the first graphs of Fig. 6(a) and Fig. 6(b), it can be seen that the result of the most important objective ΔCE in the condition of λ_1 optimized by γ-NSGA-II is lower than that of NSGA-II. And comparing the fourth graphs of Fig. 6(a) and Fig. 6(c), it can be seen that the result of the most important objective C_F in the condition of λ_2 optimized by γ-NSGA-II is lower than that of NSGA-II.

In order to further verify the impact of different optimized objectives vectors on evolutionary results, 12 rounds of genetic evolution were carried out under the above three conditions, and each of them experienced 50 generations of evolutionary iterations. For each round of genetic evolution, the average values of the individuals in the final Pareto solution set (the 50th generation) for four objectives are calculated and listed in Table 3. By observing the average of 12 rounds of genetic results, it can be seen that:

(1) In the condition of $\gamma_1 = [\Delta CE, CE_{THD}, W_F, C_F]$, the average value of the most important objective
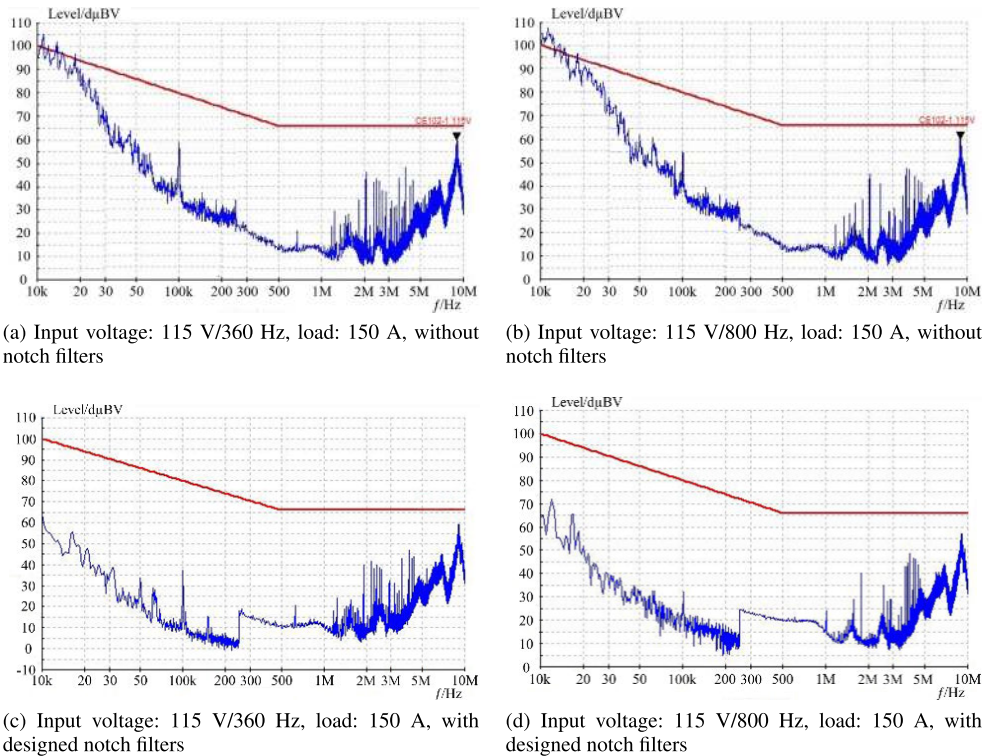
(a) Input voltage: 115 V/360 Hz, load: 150 A, without notch filters

(b) Input voltage: 115 V/800 Hz, load: 150 A, without notch filters

(c) Input voltage: 115 V/360 Hz, load: 150 A, with designed notch filters

(d) Input voltage: 115 V/800 Hz, load: 150 A, with designed notch filters

FIGURE 9. Result comparisons of EMI tests for the TRU power line.

ΔCE is 62.903, which is the lowest of the three evolutionary conditions. The average value of the least important objective C_F is 1.478, which is the highest of the three conditions.

(2) In the condition of $\gamma_2 = [C_F, \Delta CE, CE_{THD}, W_F]$, the average value of C_F is 0.937, which is the lowest of the three conditions, and the average value of W_F is 2.407, which is the highest of the three conditions.

(3) The results of the NSGA-II algorithm shows that none of its objectives are optimized to the lowest of the three conditions.

Furthermore, another comparison experiment was conducted, in which the traditional NSGA-II algorithm was used to evolve generations, and only the two most important objectives (ΔCE, CE_{THD}) were optimized. As the results of the experiment show, although the traditional NSGA-II can optimize the two objectives to a lower value, two other objectives (W_F, C_F) are not optimized at all. Their values are 3.101 and 2.712, respectively, which are evidently higher than the values from the three other comparison experiments. However, in the optimization task, W_F and C_F are also important and should be optimized, although they may be less important than the other two objectives.

The comparative analysis of the examples verifies the advantages of the developed γ-NSGA-II over NSGA-II. Firstly, the γ-NSGA-II algorithm makes the evolutionary process take the importance of objectives into account. It can reduce the value of more important objectives by sacrificing a

small part of the optimization effect of less important objectives. Also, it allows users to set the objectives importance vector γ according to the actual situation, so that the optimization results can be satisfactory in different engineering applications.

B. EXPERIMENTAL VERIFICATION

According to the importance of optimized objectives for the power supply system of C919 flight test equipment, the objective importance vectors can be obtained: $\gamma = [\Delta CE, CE_{THD}, W_F, C_F]$. The Pareto solution set shown in Table 4 is obtained by evolution using the γ-NSGA-II algorithm. There are several solutions in the Pareto solution set. The importance of each optimization objective is quite different in different applications, and the solution, which can make the most important objective reach the optimum, is preferred. Thus, in this case, the 8th group with the lowest ΔCE in Table 4 is chosen as the optimal solution, and the chromosome corresponding to the optimal solution is:

$$X = [R_1, f_1, Q_1, R_2, f_2, Q_2, R_3, f_3, Q_3]$$
$$= [4.08, 21500, 0.92, 4.06, 18200, 1.1, 4.15, 13100, 1.3]$$

(16)

According to eqs. (2) and (3), the notch filter parameters are calculated, and the nominal values are selected. The notch filter for the A phase consists of three branches, as shown in Fig. 7, in which R1 = 4.1 Ω, R2 = 4.1 Ω, R3 = 4.1 Ω,

TABLE 4. Optimization target values in Pareto solution set of γ-NSGA-II algorithm.

	ΔCE	CE_{THD}	W_{F}	C_{F}
1	62.899	3.356	2.430	1.762
2	62.946	3.356	1.710	1.230
3	62.916	3.356	2.040	1.473
4	62.915	3.356	2.057	1.486
5	62.940	3.356	1.707	1.233
6	62.900	3.356	2.429	1.758
7	62.901	3.356	2.432	1.760
8	62.878	3.356	2.417	1.770

C1 = 2 μF, C2 = 2 μF, C3 = 2 μF, L1 = 33 μH, L2 = 47 μH, L3 = 63 μH. The prototype of the 12-pulse TRU for the experiment is shown in Fig. 8(a), and the notch filters for the A, B, and C phases, which contain three notch filters shown in Fig. 7, are shown in Fig. 8(b).

EMI tests of a TRU power line with notch filters have been conducted according to EMC standard GJB152A. The test waveforms are shown in Figs. 9(c) and (d), in which the input voltage frequencies are 360 Hz and 800 Hz, respectively. For comparison, the waveforms of EMI tests of a TRU power line without notch filters are shown in Figs. 9(a) and (b), in which the input voltage frequencies are 360 Hz and 800 Hz, respectively. It can be seen from the test waveforms that after the notch filters are installed, the conducted emissions in the 10 kHz to 10 MHz frequency band have been reduced to below the standard line. The experiments show that the designed notch filters can ensure that the conducted interference meets the requirements of GJB151A.

VI. CONCLUSIONS

Based on the NSGA-II algorithm, the influence of the degree of importance of different optimized objectives on population evolution is studied. The main contributions of this article include:

The concept of the objective importance degree is introduced, and a γ-NSGA-II algorithm based on NSGA-II is developed to obtain the optimal solution for objectives with higher importance. Meanwhile, the dimensionality reduction strategy based on the objective importance vector can avoid the problem of non-uniform solution distribution caused by the crowded distance strategy of NSGA-II when there are more than two optimization objectives. They can be proved by experiments in which parameters of a notch filter for EMI suppression are optimized with ΔCE, CE_{THD}, weight, and cost as the optimization objectives. In addition, the traditional EMI test, which is time-consuming and expensive, is not reasonable for data-based analysis. In order to obtain the fitness function of the optimization objectives, a data-based conducted EMI emission model is established. As shown in section IV, the nonlinear mapping relationship between the parameters of the notch filter and ΔCE, CE_{THD} is obtained by

training the neural network, which provides a new direction for EMI evaluation modeling.

When the developed γ-NSGA-II algorithm is adopted, the number and importance of optimization objectives can be adjusted according to the characteristics and performance of the application objects. Thus, the algorithm can be widely extended to multi-objective optimization in other fields. The method of establishing fitness functions based on a BP neural network can be used to solve other nonlinear mapping relationships. The future work can be carried out from these two aspects: (1) reduce the computational complexity of the proposed γ-NSGA-II algorithm; (2) optimize the EMI evaluation model to represent the mapping relationship between notch filter parameters and EMI.

REFERENCES

[1] L. Liu, Y.-J. Liu, and S. Tong, "Neural networks-based adaptive finite-time fault-tolerant control for a class of strict-feedback switched nonlinear systems," *IEEE Trans. Cybern.*, vol. 49, no. 7, pp. 2536–2545, Jul. 2019.

[2] H. J. Liang, L. C. Zhang, Y. H. Sun, and T. W. Huang, "Containment control of semi-Markovian multiagent systems with switching topologies," *IEEE Trans. Systems, Man, Cybern., Syst.*, early access, Oct. 28, 2019, doi: 10.1109/TSMC.2019.2946248.

[3] H. Liang, Y. Zhang, T. Huang, and H. Ma, "Prescribed performance cooperative control for multiagent systems with input quantization," *IEEE Trans. Cybern.*, vol. 50, no. 5, pp. 1810–1819, May 2020.

[4] M. Mirjafari, S. Harb, and R. S. Balog, "Multiobjective optimization and topology selection for a module-integrated inverter," *IEEE Trans. Power Electron.*, vol. 30, no. 8, pp. 4219–4231, Aug. 2015.

[5] H. S. Xiao, Q. Q. Li, Y. Zhang, Z. X. Qi, B. H. Wang, and B. Liu, "Optimization of fault current limiter configuration based on improved NSGA-2," *Power Syst. Technol.*, vol. 40, no. 8, pp. 2444–2450, May 2016.

[6] J. L. Sun, S. P. Wu, and Y. C. Chen, "Optimal configuration of distributed generation in distribution network based on improved NSGA2," *Electr. Power Construct.*, vol. 35, no. 2, pp. 86–90, Feb. 2014.

[7] H. Cheng, Y. H. Gao, C. Wang, W. Q. Yang, W. G. Zhu, L. P. Peng, L. P. Luo, and X. Ao, "Multi-objective distribution network reconfiguration base on non-revisiting NSGA-II algorithm," *Power Syst. Protection Control*, vol. 44, no. 23, pp. 10–16, Dec. 2016.

[8] S. Yijie and S. Gongzhang, "Improved NSGA-II multi-objective genetic algorithm based on hybridization-encouraged mechanism," *Chin. J. Aeronaut.*, vol. 21, no. 6, pp. 540–549, Dec. 2008.

[9] L. Wang, T.-G. Wang, and Y. Luo, "Improved non-dominated sorting genetic algorithm (NSGA)-II in multi-objective optimization studies of wind turbine blades," *Appl. Math. Mech.*, vol. 32, no. 6, pp. 739–748, Jun. 2011.

[10] C. Y. Luo, M. Y. Chen, and C. Y. Zhang, "Improved NSGA-II algorithm with circular crowded sorting," *Control Decis.*, vol. 25, no. 2, pp. 227–231, Feb. 2010.

[11] H. L. Jiang, X. An, Y. W. Wang, J. Z. Qing, and G. C. Qian, "Improved NSGA2 algorithm based multi-objective planning of power grid with wind farm considering power quality," *Proc. CSEE*, vol. 35, no. 21, pp. 5405–5411, Nov. 2015.

[12] J. Chen, S. W. Xiong, and W. R. Lin, "Research on improvement strategy of NSGA-II algorithm," *Comput. Eng. Appl.*, vol. 49, no. 19, pp. 42–45, Jul. 2011.

[13] W. X. Sheng, X. S. Ye, K. Y. Liu, and X. L. Meng, "Optimal allocation between distributed generations and microgrid based on NSGA-II algorithm," *Proc. CSEE*, vol. 35, no. 18, pp. 4655–4662, Sep. 2015.

[14] K. Deb and H. Jain, "An evolutionary many-objective optimization algorithm using reference-point-based nondominated sorting approach, part I: Solving problems with box constraints," *IEEE Trans. Evol. Comput.*, vol. 18, no. 4, pp. 577–601, Aug. 2014.

[15] H. Jain and K. Deb, "An evolutionary many-objective optimization algorithm using reference-point based nondominated sorting approach, part II: Handling constraints and extending to an adaptive approach," *IEEE Trans. Evol. Comput.*, vol. 18, no. 4, pp. 602–622, Aug. 2014.

[16] D. Q. Liu, Y. N. Wang, and X. F. Yuan, "Cooperative dispatch of large-Scale electric vehicles with wind-thermal power generating system," *Trans. China Electrotech. Soc.*, vol. 32, no. 8, pp. 18–26, Feb. 2017.

[17] T. Sekine, H. Asai, and J. S. Lee, "Unified circuit modeling technique for the simulation of electrostatic discharge (ESD) injected by an ESD generator," in *Proc. IEEE Int. Symp. Electromagn. Compat.*, Pittsburgh, PA, USA, Aug. 2012, pp. 340–345.

[18] S. Caniggia and F. Maradei, "Circuit and numerical modeling of electrostatic discharge generators," *IEEE Trans. Ind. Appl.*, vol. 42, no. 6, pp. 1350–1357, Nov. 2006.

[19] H. Zhu, J.-S. Lai, A. R. Hefner, Y. Tang, and C. Chen, "Modeling-based examination of conducted EMI emissions from hard- and soft-switching PWM inverters," *IEEE Trans. Ind. Appl.*, vol. 37, no. 5, pp. 1383–1393, 2001.

[20] J.-S. Lai, X. Huang, E. Pepa, S. Chen, and T. W. Nehl, "Inverter EMI modeling and simulation methodologies," *IEEE Trans. Ind. Electron.*, vol. 53, no. 3, pp. 736–744, Jun. 2006.

[21] X. Huang, E. Pepa, J.-S. Lai, S. Chen, and T. W. Nehl, "Three-phase inverter differential mode EMI modeling and prediction in frequency domain," in *Proc. 38th IAS Annu. Meeting Conf. Rec. Ind. Appl. Conf.*, Salt Lake City, UT, USA, 2003, pp. 2048–2055.

[22] J. Meng, W. M. Ma, L. Zhang, and Z. H. Zhao, "EMI evaluation of power converters considering IGBT switching transient modeling," *Proc. CSEE*, vol. 25, no. 20, pp. 16–20, Oct. 2005.

[23] F. Xiao and L. Sun, "Conducted electromagnetic interference prediction for power converters under variable switching conditions," *Proc. CSEE*, vol. 33, no. 3, pp. 176–183, Dec. 2013.

[24] Q. Wu and M. Wei, "A mathematical expression for air ESD current waveform using BP neural network," *J. Electrostatics*, vol. 71, no. 2, pp. 125–129, Apr. 2013.

[25] Y. M. Li, Y. J. Zhu, X. Li, J. H. Yu, and Q. D. Wang, "Artificial neural networks-based prediction of electromagnetic compatibility problems," *J. Chongqing Univ.*, vol. 31, no. 11, pp. 1313–1316, Nov. 2008.

[26] C. L. Zhou, Z. Y. Wang, T. Liu, S. G. Zhao, and Z. H. Liang, "Low dropout linear regulator's electromagnetic interference damage model based on BP neural network," *High Voltage Eng.*, vol. 42, no. 3, pp. 973–979, Apr. 2016.

[27] Z. M. Qian and H. L. Chen, "State of art of electromagnetic compatibility research on power electronic equipment," *Trans. China Electrotechnical Soc.*, no. 7, pp. 1–11, Jul. 2007.

[28] S. S. Wang, M. Gong, and Z. Song, "Predicting the suppression effect of EMI filter based on the S-parameter method," *Trans. China Electrotech. Soc.*, vol. 31, no. 18, pp. 66–74, Sep. 2016.

[29] Y.-P. Chang and C.-N. Ko, "A PSO method with nonlinear time-varying evolution based on neural network for design of optimal harmonic filters," *Expert Syst. Appl.*, vol. 36, no. 3, pp. 6809–6816, Apr. 2009.

[30] X. L. Lu, L. W. Zhou, S. H. Zhang, and C. K. Cao, "Multi-objective optimal design of passive power filter," *High Voltage Eng.*, vol. 33, no. 12, pp. 177–182, Dec. 2007.

[31] *Measurement of Electromagnetic Emission and Susceptibility for Military Equipment and Subsystems*, Standard GJB 152A, 1997.

[32] Y. C. Zhang, S. B. Ye, J. J. Zhang, and Y. T. Yao, "Review of conducted noise suppression method for power electronic and electrical equipment," *Trans. China Electrotech. Soc.*, vol. 32, no. 14, pp. 77–86, Jul. 2017.

[33] Q. D. Wang, Z. Y. An, Y. L. Zheng, H. M. Peng, and X. Li, "Electromagnetic compatibility optimization design for switching power supply used in electric vehicle," *Trans. China Electrotech. Soc.*, vol. 29, no. 9, pp. 225–231, Sep. 2014.

[34] X. L. Lu, S. H. Zhang, L. W. Zhou, and C. K. Cao, "Multi-objective optimal design and experimental simulation for passive power filters," *East China Electr. Power*, vol. 35, no. 4, pp. 29–32, Apr. 2007.

• • •